Current Zoology, 2023, **69**, 442–455
https://doi.org/10.1093/cz/zoac061
Advance access publication 10 August 2022
Original Article

Phylogeography of the desert scorpion illuminates a route out of Central Asia

Cheng-Min SHI[a,*], Xue-Shu ZHANG[b], Lin LIU[b], Ya-Jie JI[b], and De-Xing ZHANG[b,c,*]

[a]State Key Laboratory of North China Crop Improvement and Regulation, College of Plant Protection, Hebei Agricultural University, Baoding 071001, China
[b]State Key Laboratory of Integrated Management of Pest Insects and Rodents, Institute of Zoology, Chinese Academy of Sciences, Beijing 100101, China
[c]University of Chinese Academy of Sciences, 19 Yuquan Road, Beijing 100049, China

[*]Address correspondence to Cheng-Min Shi. E-mail: shichengmin@hebau.edu.cn; De-Xing Zhang. E-mail: dxzhang@ioz.ac.cn
Handling editor: Zhi-Yun JIA

Abstract

A comprehensive understanding of phylogeography requires the integration of knowledge across different organisms, ecosystems, and geographic regions. However, a critical knowledge gap exists in the arid biota of the vast Asian drylands. To narrow this gap, here we test an "out-of-Central Asia" hypothesis for the desert scorpion *Mesobuthus mongolicus* by combining Bayesian phylogeographic reconstruction and ecological niche modeling. Phylogenetic analyses of one mitochondrial and three nuclear loci and molecular dating revealed that *M. mongolicus* represents a coherent lineage that diverged from its most closely related lineage in Central Asia about 1.36 Ma and underwent radiation ever since. Bayesian phylogeographic reconstruction indicated that the ancestral population dispersed from Central Asia gradually eastward to the Gobi region via the Junggar Basin, suggesting that the Junggar Basin has severed as a corridor for Quaternary faunal exchange between Central Asia and East Asia. Two major dispersal events occurred probably during interglacial periods (around 0.8 and 0.4 Ma, respectively) when climatic conditions were analogous to present-day status, under which the scorpion achieved its maximum distributional range. *M. mongolicus* underwent demographic expansion during the Last Glacial Maximum, although the predicted distributional areas were smaller than those at present and during the Last Interglacial. Development of desert ecosystems in northwest China incurred by intensified aridification might have opened up empty habitats that sustained population expansion. Our results extend the spatiotemporal dimensions of trans-Eurasia faunal exchange and suggest that species' adaptation is an important determinant of their phylogeographic and demographic responses to climate changes.

Key words: aridification, ecological niche modeling, drylands, *Mesobuthus*, Pleistocene, population expansion

Phylogeography emerges as a fundamental branch of biogeography and evolutionary genetics. It provides a powerful tool for deciphering the factors and processes that have shaped the spatial distribution of genetic variation within and among closely related taxa in geo-climatic contexts (Knowles 2009). Numerous phylogeographic studies have repeatedly demonstrated that past climatic oscillations have triggered recurrent reorganizations of biota at all levels and scales, from genes to ecosystems (Hewitt 2000; Davis and Shaw 2001). Given a certain climatic event, it can either pose a threat or provide an opportunity depending on the species' genetic, physiological and behavioral adaptational profiles (Garcia et al. 2014). Thus, species respond to climatic change in individualistic ways (Hewitt 2000; Willis et al. 2004; Ackerly et al. 2010; Anadón et al. 2015). Besides, historical climate changes were expressed variably across geographic locations (Hewitt 2000) and their impacts were unfolded in multiple dimensions (Garcia et al. 2014). These features make comprehension of phylogeographic histories a very complex issue that requires integrating information from diverse organisms, ecosystems, geographic regions, and climate regimes. However, phylogeographic studies are biased toward the temperate regions of Europe and North America and focused predominantly on the impact of glaciations (Keppel et al. 2012). Our knowledge of phylogeography in drylands is still very limited, where aridification, a more widespread coeval of the Quaternary glaciation, has played a dominant role (Byrne et al. 2008, 2018; Shi et al. 2013; Maestre et al. 2021).

Drylands, covering about 41% of Earth's land surface (Reynolds et al. 2007), constitute the largest terrestrial biome on the planet (Schimel 2010) and provide a crucial share of ecosystem services to the fast-growing human population (Wang et al. 2014). They are among the most sensitive and fragile ecosystems on Earth (Austin 2011) and face a high risk of degradation due to various threats including climate change (Reynolds et al. 2007; Tietjen et al. 2010). Without any doubt, drylands represent the main field for mitigating challenges imposed by global climate changes. As understanding the biotic response to past challenges provides a compass for contemporary and future challenges (Avise et al. 2016), knowing how dryland organisms have evolved and responded to the past climate not only provides insights into their resilience and ability to adapt to climate changes but also informs us of the way we can effectively mitigate future climate changes

Received 16 June 2022; accepted 27 July 2022

(Byrne et al. 2008; Pepper and Keogh 2021). However, such knowledge is particularly scarce in Asian drylands.

Arid Central Asia (ACA) represents the largest non-zonal temperate dryland in the world, stretching the mid-latitude Eurasian continent and encompassing the Central Asian countries, northwest China and Mongolia (Chen et al. 2016). Aridification in Central Asia traced back to the Eocene-Oligocene boundary about 34 million years ago (Ma) (Sun and Windley 2015) and has been the surrogate of climatic changes and profoundly modulated the evolution of biota ever since (Guo et al. 2002; Bougeois et al. 2018). Fossil records indicate that concurrent with increasing aridification, a single cohesive Old World savannah palaeobiome once emerged in mid-latitude Eurasia during the Neogene (Kaya et al. 2018). The palaeobiome flourished under the influence of the Miocene global cooling and regional aridification and reached its peak extent between 6 and 9 Ma when the arid steppe climate in East Asia was more widespread and better connected to those in western Asia (Kaya et al. 2018). During this period, ACA appeared to be a crossroad for biotic exchange between West and East Asia. The uplift of the Tian Shan during the Neogene and the confluence of the southern Tian Shan range and Pamir around the Miocene-Pliocene boundary formed a prominent barrier and divided the ACA into two distinct zoographical subregions (Charreau et al. 2009; Sun et al. 2015). The Central Asia (CA) subregion in the west ranges from the east bank of the Caspian Sea to the west of the Tian Shan-Pamir ranges, and the Gobi subregion (*sensus* Mongolian Plateau by He et al. 2020) in the east encompasses northwest China and southern Mongolia (Kreft and Jetz 2010; Holt et al. 2013; He et al. 2020). Such a zoogeographic configuration highlights that the Tian Shan-Pamir ranges have played an important vicariant role within ACA and impeded biotic exchange between the CA and Gobi subregions (Barbolini et al. 2020; He et al. 2020). However, trans-ACA distributions of some closely related arid species/lineages (e.g. *Mesobuthus* scorpions, Shi et al. 2013; *Eremias* lizards, Liu et al. 2019) also signify the crucial role of dispersal in modulating Quaternary phylogeography and extant distribution. Meanwhile, the geo-climatic context for the formation of post-uplift trans-ACA distributions remains enigmatic, and the dispersal routes that have connected the CA and Gobi subregions, or West Asia and East Asia in general, still await to be defined.

Owing to their extraordinary biology and ecology, scorpions become a promising model for biogeographic studies in historical geo-climatic context (Bryson et al. 2013a; Shi et al. 2013; Ceccarelli et al. 2016; Dolby et al. 2019), especially for various drylands in Central Asia (Graham et al. 2012, 2019), Middle East (Alqahtani et al. 2022), North Africa (Cain et al. 2021), southwestern North America (Bryson et al. 2013b; Graham et al. 2013a, b; Miller et al. 2014), and South American Pacific Coast (Ceccarelli et al. 2017). They represent an iconic and charismatic lineage of arthropods (Sharma et al. 2015), well known for some of their unique biological characteristics, including morphological conservatism (Sissom 1990), low resting metabolic rate (McCormick and Polis 1990; Wang et al. 2019), and unusual life history that are more similar to those of long-lived vertebrates (Gantenbein and Largiadèr 2002). These features collectively enable scorpions to survive the drastic environmental changes and mass extinctions over the past 425 million years (Polis 1990). Among them, the genus *Mesobuthus* Vachon, 1950 appears to be particularly suitable for studying the biogeography of Eurasian drylands. *Mesobuthus* (*sensu* Gantenbein et al. 2003) includes several species complexes spreading widely in the mid-latitude steppe-desert biome (Fet 1994; Fet et al. 2000). Their distribution strides west-east in tandem from the Mediterranean to east China, and mirrors a trans-Eurasian section of climate types. This group may have originated in West Asia (Anatolia) in the mid-Miocene (Shi et al. 2013), and since then undergone extensive diversification and biogeographic evolution driven by regional tectonics (Mirshamsi et al. 2010, 2011) and climate changes (Shi et al. 2013), which gave rise to more than 30 species with Central Asia being the center of diversity (Fet et al. 2000, 2018, 2021; Graham et al. 2019; Kovařík 2019). A recent revision of the genus described additional 14 new species (Kovařík et al. 2022). Currently, at least five species occur to the east of the Tian Shan-Pamir ranges in China and Mongolia (Shi and Zhang 2005; Shi et al. 2007; Di et al. 2014; Fet et al. 2018; Zhang et al. 2020). The varying divergences among these species/lineages provide opportunities for testing biogeographical hypotheses in geo-climatic contexts with varying spatial and temporal scales.

It has been hypothesized that *Mesobuthus* scorpions colonized East Asia through multiple waves of west-to-east dispersals out of Central Asia (Shi et al. 2013). However, the exact routes and the geo-climatic contexts that facilitated these dispersals remain to be defined. Here, we test an "out-of-Central Asia" hypothesis for the desert scorpion *Mesobuthus mongolicus* (Birula, 1911) by defining its dispersal routes and demographic history in the Quaternary through an integrated approach combining Bayesian phylogeographic reconstruction and ecological niche modeling. This scorpion was formerly known as *M. eupeus mongolicus* and has recently been upgraded to an independent species (Kovařík 2019). It represents the easternmost member of the *M. eupeus* complex (Shi et al. 2015a; Fet et al. 2018). The Gobi population of *M. mongolicus* has been proposed as a product of the out-of-Central Asia move of its ancestors during the late Pleistocene (Shi et al. 2013). In the present study, we addressed the phylogeography of *M. mongolicus* by focusing on the following two questions: (1) where and when did the desert scorpion originate and (2) how have climatic forces shaped the route for out-of-Central Asia dispersal during the Quaternary? Given scorpions are generalist predators and exist at an intermediate level of food chains (McCormick and Polis 1990), the insights gained from the desert scorpion *M. mongolicus* could provide a reference for other arid animals in Asian drylands in general.

Materials and Methods

Sample collection and genetic data

Surveys of scorpion fauna in China and adjacent regions have been conducted since 2005. Specimens of *M. mongolicus* were collected from a total of 51 localities across its potential geographical range (Shi et al. 2015a). These localities include 41 sites in China (C_1–C_{41}), 8 sites in Mongolia (M_1–M_8), and one site each in Tajikistan (TJ1) and Kazakhstan (KZ1, Figure 1 and Supplementary Table S1). All specimens from China and Mongolia were collected by the authors. Specimens from Tajikistan were provided courtesy of Dr. Hongbin Liang and specimens from Kazakhstan were provided by Mr. Alexander V. Gromov. Genomic DNA was extracted using a modified

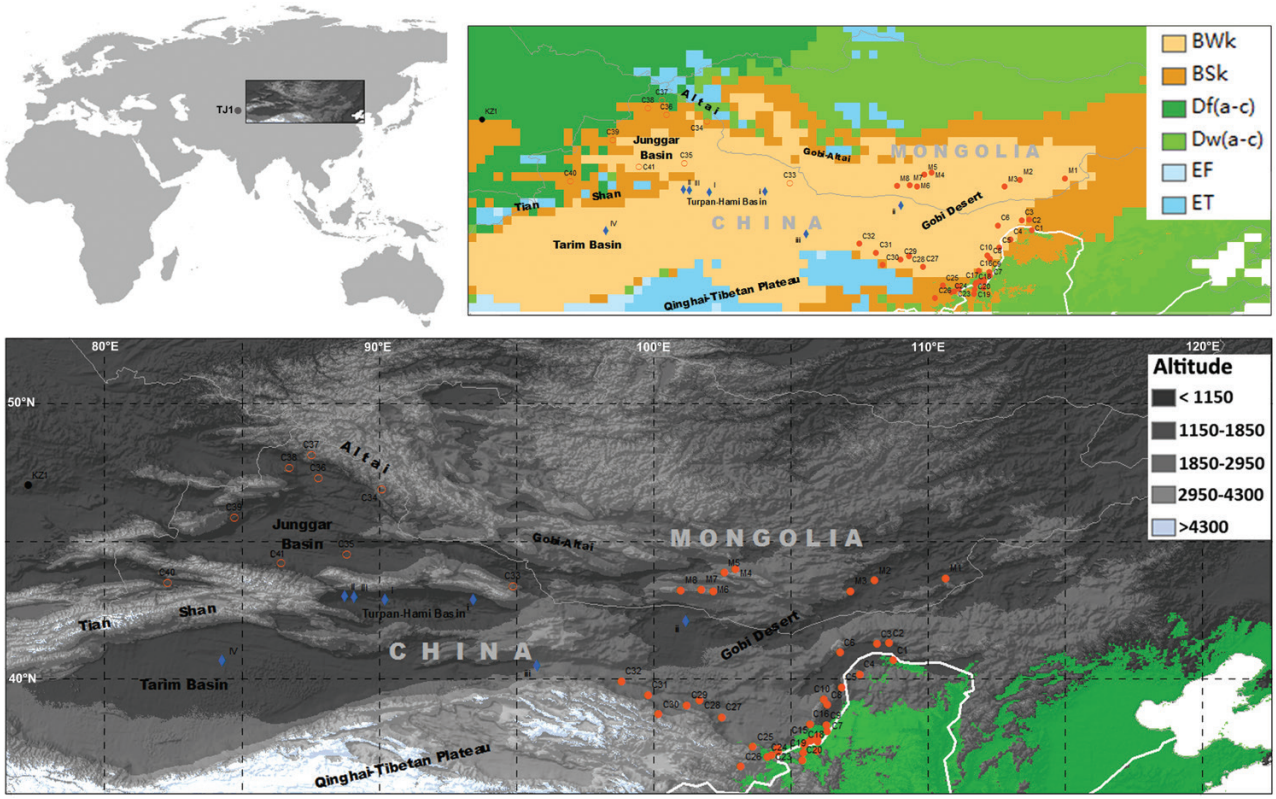

Figure 1. Geographic sampling of the desert scorpion *M. mongolicus*. The sampled sites were plotted on the digital elevation map (bottom, source data from Fick and Hijmans 2017) and the map of Köppen-Geiger climatic classification (top right, source data from Peel et al. 2007) of the studied areas. The maps were edited and illustrated using QGIS (https://www.qgis.org/en/site/). BWk: arid, desert, cold; BSk: arid, steppe, cold; Df(a–c): cold, without dry season; Dw(a–c) cold, dry winter; EF: polar, frost; ET: polar, tundra. Orange dots, the Gobi population of *M. mongolicus*; orange circles, the Junggar population of *M. mongolicus*; blue diamonds, *M. prezwalskii*. *M. mongolicus* and *M. prezwalskii* are typical arid species occurring widely in arid ecosystems (BWk and BSk). The green area in the low right on the elevation map represents the potentially suitable distributional areas of *M. martensii*.

phenol-chloroform extraction procedure (Zhang and Hewitt 1998). Voucher specimens and DNA extracts were deposited at the Laboratory of Molecular Ecology and Evolution, Institute of Zoology (MEE-IOZ), Chinese Academy of Sciences.

Sequences for the mitochondrial cytochrome *C* oxidase subunit I (mtCOI) gene and three nuclear loci (nuclear protein kinase, PK; Serin-type endopeptidase, STE and Serin proteinase inhibitor, Spn2) were sequenced using the primers and protocols of Shi et al. (2013). For the mtCOI dataset, 297 individuals of *M. mongolicus* were sequenced in the present study, and were combined with 45 individuals from the study by Shi et al. (2013), making up a dataset of a total of 342 sequences from China (N = 278), Mongolia (N = 62), Tajikistan (N = 1) and Kazakhstan (N = 1). The sample sizes ranged from 1 to 16 individuals. Given the low intraspecific genetic diversity (Shi et al. 2013), only one individual from each of the 15 selected sites was analyzed for PK, STE and Spn2 (Supplementary Table S1). These three nuclear loci were also sequenced for 8 individuals of *M. przewalskii*. New sequences have been deposited in GenBank under accession numbers of OP022642-OP022704 for mtDNA haplotypes (Supplementary Table S2), OP019756-OP019778 for PK sequences, OP019779-OP019801 for Spn2 sequences and OP019802-OP019824 for STE sequences (Supplementary Tables S3 and S4).

Phylogenetic analyses and divergent time estimate

Sequences were aligned using MUSCLE (Edgar 2004). Given the mitochondrial genome and nuclear genome undergo different modes of inheritance and evolution, the mtCOI sequences and the nuclear loci (PK, STE and Spn2) were analyzed separately. We determined the unique haplotypes using DnaSP version 6.12.03 (Rozas et al. 2017). The total 342 mtCOI sequences collapsed into 65 unique haplotypes (612 bp in length), of which one haplotype was from Tajikistan (TJ01), one haplotype was from Kazakhstan (KZ01), and all other 63 haplotypes were from northwest China and south Mongolia (Supplementary Table S2). Combined with 12 samples of *M. przewalskii* (Zhang et al. 2020), 10 samples of *M. martensii* (Shi et al. 2013), 6 representatives for three other species of *M. eupeus* complex (Mirshamsi et al. 2010) and two outgroups (*Androctonus australis* and *Buthus occitanus*), the final dataset includes 95 unique mtCOI sequences (Supplementary Table S3). The GTR + Γ model was selected as the best-fit model by Modeltest 3.7 program (Posada and Crandall 1998) according to the Akaike information criterion. Maximum likelihood (ML) analysis was carried out using PhyML 3.0 (Guindon et al. 2010) with SPR tree search operation. Topological robustness was assessed through bootstrapping with 1000 replicates. Bayesian analysis was carried out with MrBayes 3.2 (Ronquist et al. 2012). Analyses were initiated with random starting trees and run for 5×10^6 generations with four Markov chains employed. Trees were sampled every 500 generations and the 'temperature' parameter was set to 0.2. The first 30% of trees were discarded as burn-in after checking for stationarity and convergence. Median-joining network (Bandelt et al. 1999) was constructed using Network 4.6.1.2 (http://www.fluxus-engineering.com/) to visualize intraspecific relationships among distinct haplotypes.

For the three nuclear loci (PK, 340 bp; STE, 360 bp; and Spn2, 366 bp), phylogenetic analyses were performed on the concatenated matrix because each gene individually harbored poor genetic variations. The concatenated matrix included a total of 1066 sites from 36 samples belonging to five species (*M. mongolicus*, 15; *M. przewalskii*, 8; *M. martensii*, 11; *M. cyprius* 1; *M. gibbosus*, 1; Supplementary Table S4). The TrN model was selected as the best-fit model, and all other settings in ML analysis were the same as those used in the analyses of the mtCOI dataset. MrBayes was run for 1×10^6 generations with trees and parameters sampled every 100 generations.

Divergence time was estimated from mtCOI sequences with a relaxed molecular clock approach implemented in BEAST 1.10.4 (Suchard et al. 2018). We combined the most diverged mtCOI haplotypes revealed here with our previous alignment into a new dataset with 53 sequences and estimated divergent times with the same calibrating method (Shi et al. 2013). The rate change was explicitly modeled using uncorrelated log-normal distribution across the tree. Using the GTR + Γ model and a Yule process for speciation prior, we performed 100 million Markov chain Monte Carlo (MCMC) searches, sampling once every 1000 generations. Stationarity and the convergence of the MCMC chains were checked with Tracer 1.7 (Rambaut et al. 2018). Maximum clade credibility (MCC) tree, posteriors, means and 95% highest posterior densities (HPDs) of ages for nodes were identified and annotated using TreeAnnotator 1.10 (Suchard et al. 2018).

Phylogeographic diffusion in continuous space

Phylogeographic reconstruction was only based on the mtCOI data due to limited spatial sampling and low genetic variation of the nuclear genes. Current and predicted suitable distribution area of *M. mongolicus* stretches continuously across the entire studied region (Shi et al. 2015a). There are no obvious potential barriers that can be enrolled to define discrete areas, and thus it is arbitrary to divide species range into discrete operational areas *a priori*. Therefore, we inferred spatial diffusion of genealogies using a continuous Bayesian phylogeographic method which models the geographic spread of genealogies across spaces with continuous diffusion processes conditioned on sampling location defined as bivariate traits representing latitude and longitude for each accession (Lemey et al. 2010). We first selected the best-fit diffusion model by performing marginal likelihood estimation using generalized stepping-stone sampling on three available relaxed random walk models, as well as the time-homogeneous Brownian motion process. The Bayesian phylogeographic diffusion analysis was performed using BEAST v. 1.10.4 (Suchard et al. 2018). MCMC were run for 50 million generations with trees and parameters sampled every 5,000 generations. MCMC samples were summarized using TreeAnnotator. The results of phylogeographic reconstruction were visualized in SpreaD3 (Bielejec et al. 2016).

Demographic inferences

Historical changes in the effective population size were assessed using mtCOI data by employing two approaches. First, we used summary statistic tests, *D* (Tajima 1989), *Fs* (Fu 1997) and R_2 (Ramos-Onsins and Rozas 2002). Tajima's *D* test is based on the number of segregating sites, Fu's *Fs* test uses information from the haplotype distribution, while Ramos-Onsins and Rozas's R_2 test uses information on the mutation frequency. These statistics have high power to detect population expansion for non-recombining regions of the genome under a variety of different circumstances, either when the sample size is large (*Fs*) or when the sample size is small (*D*), and the number of segregating sites is low (R_2). The significance of each test was assessed by generating null distribution from 10,000 coalescent simulations in DnaSP version 6.12.03 (Rozas et al. 2017). Significantly large negative *D* and *Fs* values and significantly positive R_2 values were taken as evidence of population expansion. Second, the effective population size at different points along the genealogical timescale was explored by coalescent-based Bayesian skyline plots (BSPs) using BEAST 1.10.4 (Suchard et al. 2018). Unlike the above tests which are based on summary statistics, BSP makes use of all the historical information contained within a sample of DNA sequences from a given population. BSP assumes DNA sequences have been randomly sampled from across the range of a panmictic population (Ho and Shapiro 2011). We performed BSP analysis on mtCOI sequences of *M. mongolicus* from China and Mongolia (N = 340) but excluded the divergent sequence (TJ01) from Tajikistan, which might violate the assumption of panmixia. Population structure is known to result in biased estimates of model parameters which in turn can produce patterns in the demographic plot other than changes in the overall population size (Pannell 2003; Strimmer and Pybus 2001). No mtCOI haplotype was shared between the Junggar population and the Gobi population. This signifies the existence of population structure. Therefore, we also performed BSP analyses for the Junggar population and the Gobi population independently. The evolutionary rate estimated from molecular dating was used to calibrate BSP analyses. We ran the analysis for 5×10^8 iterations with genealogies and model parameters being sampled every 5,000 generations after discarding the first 10% iterations as burn-in.

Ecological niche modeling

Ecological niche modeling (ENM) was performed with MaxEnt version 3.3.3k (Phillips et al. 2006) based on occurrence-only records of *M. mongolicus*. Following the practical guide to MaxEnt (Merow et al. 2013), we removed localities that were within distances of 30 km from each other in the original 89 occurrence records to reduce the effect of sampling bias. The final distribution models were built based on 74 less-biased occurrence points (Supplementary Table S5). We used the bioclimatic variables for the present, the Mid Holocene (ca. 6,000 years ago), the Last Glacial Maximum (LGM, ca. 22,000 years ago) and the Last Interglacial (LIG, ca. 120,000–140,000 years ago) downloaded from WorldClim 1.4 (Hijmans et al. 2005). All the data include 19 bioclimatic variable layers at a spatial resolution of 2.5 arc-minute resolution (ca. 5 × 5 km) except those for the LIG. The original data for the LIG at 30 arc-second resolution was resampled to 2.5 arc-minute resolution before being used for model projection. The bioclimatic layers were masked to regions spanning from 35 to 55 °N and from 75 to 115 °E to avoid sampling unrealistic background data and thus inflating the strength of predictions. We used the variance inflation factor (VIF) to detect collinearity between predictor variables using usdm package (Naimi et al. 2014) in R (R Development Core Team). VIF is recommended for assessing collinearity and a value greater than 10 signifies a collinearity problem (Dormann et al. 2013). Thus, bioclimatic variables with

VIF values greater than 10 were excluded to minimize correlation among predictors and to improve the reliability of the generated models (Merow et al. 2013). Seven climatic variables, mean temperature diurnal range (BIO2), temperature seasonality (BIO4), mean temperature of the wettest quarter (BIO8), mean temperature of the driest quarter (BIO9), precipitation of the wettest month (BIO13), precipitation of the driest month (BIO14), and precipitation seasonality (BIO15) were selected for final ecological niche modeling. MaxEnt was run with a convergence threshold of 10^{-5} and a maximum number of iterations of 10,000 with 25% of localities for model testing for 10 replicates with subsample. The model was projected to past conditions with clamping. Model performance was assessed via the area under the ROC (receiver operating characteristic) curve (AUC) statistic and the importance of variables was assessed by jackknife tests. Values of AUC between 0.70 and 0.90 indicate reasonable predictions, and >0.90 indicate very good predictions (Swets 1988; Peterson et al. 2011). We employed the maximum training sensitivity plus specificity threshold (MTSS) to convert continuous models to binary predictions. The MTSS is considered to most accurately predict presence/absence (Jiménez-Valverde and Lobo 2007).

Results

Phylogenetic relationships and divergence times

The results of ML analysis and Bayesian inference were highly congruent. The ML phylogeny inferred from mtCOI dataset is shown in Figure 2A. All samples of *M. mongolicus* from China and Mongolia clustered within an unresolved star clade with reasonable support (68/0.97 for ML/Bayesian, respectively), which coalesced with TJ01 from Tajikistan with strong supports (95/1.00). We recognized this clade putatively as *M. mongolicus*. Within the *M. mongolicus* clade, all haplotypes except one from the Junggar Basin (Xinjiang) formed a sub-lineage but was not well supported. This result was mirrored by the haplotype network analysis. Haplotypes from the Junggar Basin were closely related to those from the Gobi region but no haplotype was shared between the two regions (Figure 2B, Supplementary Table S2). The *M. mongolicus* clade coalesced with KZ01 and then *M. thersites* and *M. phillipsi*, forming a monophyletic branch (71/0.99) including exclusively members of the *M. eupeus* species complex. Monophyly for both *M. prezwalskii* and *M. martensii* was strongly supported. These two species were more closely related to each other than to any member of the *M. eupeus* complex.

The result of phylogenetic analyses of the concatenated matrix for three nuclear loci (PK, STE, and Spn2) is shown in Figure 2C. As far as the interspecies relationship was concerned, the nuclear gene phylogeny was congruent with the mitochondrial phylogeny. However, a clear conflict occurred between the nuclear and the mitochondrial trees in terms of the phylogenetic relationships among lineages of *M. mongolicus*. Two moderately supported subclades were observed in the nuclear tree. One subclade (55/0.91) includes all samples from the Gobi region and three clustered samples from the Junggar Basin. The other subclade (57/0.85) includes three samples from the Junggar Basin and TJ01 from Tajikistan. Nevertheless, the monophyly of *M. mongolicus* was strongly supported (98/0.99).

The results of divergence time estimated from mtCOI data were summarized in Table 1. The time of the most recent common ancestor of *M. mongolicus* was estimated to be 1.36 Ma (95% HPD, 0.78–1.97 Ma) and the Junggar-Gobi lineage coalesced at 0.54 Ma (0.30–0.80 Ma). The divergence time between *M. mongolicus* and KZ01 was 3.37 Ma (2.12–4.54 Ma), while that between *M. prezwalskii* and *M. martensii* was 6.27 Ma (4.35–8.37 Ma). A further split within *M. prezwalskii* occurred at 1.00 Ma (0.56–1.51 Ma). The divergence between the *M. eupeus* complex and the *M. prezwalskii-M. martensii* clade occurred around 10.56 Ma (8.33–12.70 Ma).

The spatiotemporal diffusion of *M. mongolicus*

The Cauchy random walk model was selected as the best-fit diffusion model for mitochondrial lineages of *M. mongolicus*. The result of Bayesian phylogeographic reconstruction of ancestral distribution and spatial diffusion of genealogies through time supports that *M. mongolicus* originated in Central Asia and dispersed eastward step by step, and finally to the Gobi region. Three snapshots illustrating the major phylogeographic dispersal events are shown in Figure 3. The inferred ancestral distribution for the most recent common ancestors of *M. mongolicus* was located in an area to the northwest of the Tian Shan, somewhere near the boundary between Tajikistan and Kazakhstan. The ancestral population moved eastward and reached the Junggar Basin around 0.8 Ma, and then underwent regional expansion within the Junggar Basin. Around 0.4 Ma, *M. mongolicus* dispersed further east to the southern part of the Gobi, followed by another regional expansion in areas near the Tengger Desert and the Badain Jaran Desert, striding Gansu, Inner Mongolia and Ningxia. It was a very recent event (<0.2 Ma) that *M. mongolicus* population expanded northward to the Gobi region of southern Mongolia. During this time, a northward expansion event also occurred in the Junggar Basin which gave rise to the Altay population. It appeared that regional population expansions have persisted until the present day, which gives rise to the current trans-Gobi distribution for this species.

Demographic history

The population genetic statistics for *M. mongolicus* were summarized in Table 2. The genetic diversity of the Junggar population is higher than that of the Gobi population (0.8063 vs. 0.6849 for Hd, and 0.0029 vs. 0.0020 for π), although the sample size of the former is much smaller than the latter (23 vs. 317). Treating all samples of *M. mongolicus* as a single population or only considering the Gobi population, the values for Tajima's *D*, and Fu's *Fs* were negative and significant, and the values of Ramos-Onsins and Rozas' R_2 were small (0.0760 and 0.0769, respectively), positive and significant, suggesting demographic expansions. For the Junggar population, both the values for Tajima's *D* and Fu's *Fs* were negative but not significant, and the value of Ramos-Onsins and Rozas' R_2 was significant but much larger (0.1378), implying stable demographic history.

The variations of effective population sizes through time are shown by BSPs in Figure 4. For *M. mongolicus*, the curve of BSP can be visually divided into three phases. Before 35 thousand years ago (ka), the population was stable. From

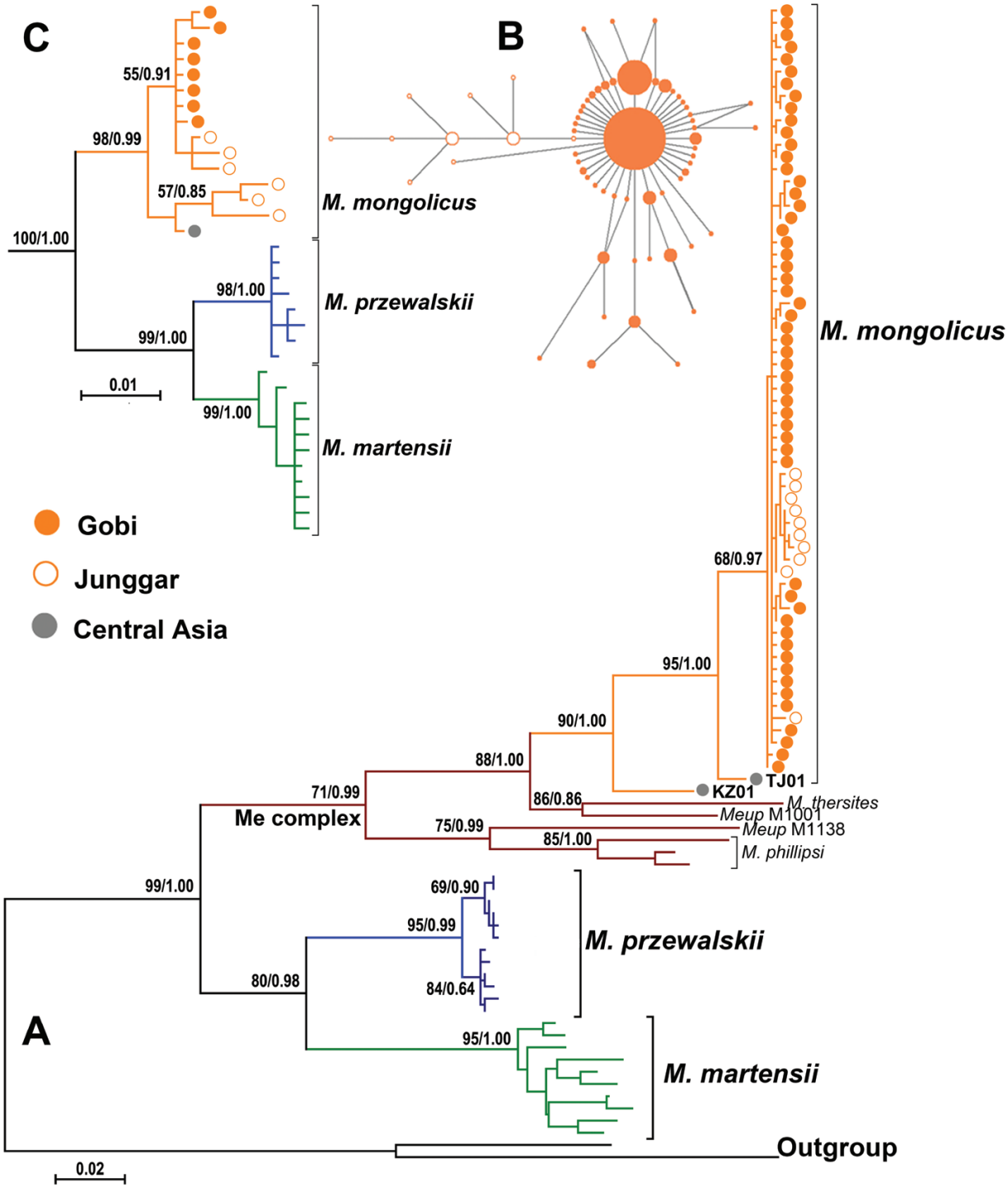

Figure 2. Phylogenetic position of the desert scorpion *M. mongolicus,* the most derived lineage of the *M. eupeus* species complex. (A) The maximum likelihood tree inferred from the mitochondrial cytochrome oxidase I (mtCOI) data. (B) Median-joining network of *M. mongolicus* mtCOI haplotypes. Branch lengths are proportional to the number of substitutions that occurred between haplotypes, and circle sizes proportional to the number of individuals bearing the haplotypes. (C) The maximum likelihood tree inferred from concatenated sequences of the three nuclear genes (PK, STE, and Spn2). Numbers at the nodes represent the bootstrap support values and Bayesian posterior probabilities. Me complex, *M. eupeus* species complex.

30 to 10 ka, population size increased sharply, even during the LGM around 21 ka. From 10 ka until to present, the BSP curve gradually plateaued off (Figure 4A). A similar BSP curve was recovered when analyzing the Gobi population only (Figure 4B) and population size increase during the LGM was also confirmed. The population size of the Junggar population appeared much more stable than the Gobi population, which increased very slightly over the past 60 kya (Figure 4C).

Temporal changes of suitable distributional areas

The distributional models generated with non-collinear (VIFs ≤ 4.60) climatic variables maintained fairly high accuracy (AUC = 0.90 ± 0.02). Of the seven climate variables used,

Table 1. Means and 95% highest posterior density intervals of divergence times estimated from mtCOI data

MRCA	Mean	95%HPD lower	95%HPD upper
M. mongolicus -KZ01	3.27	2.12	4.54
M. mongolicus	1.36	0.78	1.97
Junggar-Gobi lineage	0.54	0.30	0.80
M. prezwalskii	1.00	0.56	1.51
M. prezwalskii-M. martensii	6.27	4.35	8.37
M. mongolicus-M. martensii	10.56	8.33	12.70

Notes: The divergence times were estimated using a relaxed molecular clock approach. Means and their corresponding 95% highest posterior density (HPD) intervals for ages of the most recent common ancestor are given in million years.

BIO13 contributed to the models most with a mean relative contribution of 37.4 %, flowed by BIO9 (32.9%), and BIO8 (19.6%). The other four remaining variables collectively contributed 10.1% to the model (Supplementary Table S6). The potential distributions of *M. mongolicus* for the present, the Mid Holocene, the LGM, and the LIG were averaged over 10 models (Figure 5). The present suitable distributional area for *M. mongolicus* encompassed two major parts connected by a narrow stretching belt (Figure 5A). The western part included the entire Junggar Basin flanking by the Tian Shan Mountains in the south and the Altai Mountains in the northwest. The eastern part encompassed the Gobi Desert striding the China-Mongolia border, the Badain Jaran and Tengger Deserts, and the west edge of the Loess Plateau. The connecting belt stretched southeastward from the eastern extreme of the Junggar Basin to the Badian Jaran Desert along the Hexi Corridor at the northern edge of the Qinghai-Tibetan Plateau. The northern rim of the Tarim Basin and the eastern part of the Qaidam Basin were also potentially suitable for distribution, but *M. mongolicus* was never found in those regions (Shi et al. 2007; Shi et al. 2015a). It was clear that both the Tian Shan and Altai mountains are unsuitable areas for this species.

The projected distributional areas at the Mid Holocene, the LGM and the LIG were all contracted in comparison with the current range, with the eastern part and the western part disjointed (Figure 5B–D). In the Mid Holocene, the potentially suitable distributional (PSD) areas were only slightly contracted at the northern edge of the Gobi region but were significantly contracted in the Junggar Basin with its northeast region becoming completely unsuitable for the scorpion (Figure 5B). The most drastic contraction of PSD areas was witnessed at the LGM when most parts of the Gobi Desert and the Junggar Basin became unsuitable. The major PSD areas remained in the southwestern part of the Junggar Basin and the Badain Jaran-Tengger Deserts (Figure 5C). An obvious southeastward retreat of the PSD areas toward the Loss Plateau occurred at this time. At the LIG, most parts of the Junggar Basin were unsuitable for the species, with only a small PSD area remained at the southern rim of the basin (Figure 5D). However, a large PSD area in the east existed, encompassing the Hexi Corridor, the Badain Jaran-Tengger Deserts, the southern Gobi and most of the Loess Plateau, extending well beyond the eastern limit of the current range of *M. mongolicus*. Noticeably, the Mongolian Gobi was unsuitable for the scorpion during the LIG.

Discussion

This study contributes to dryland phylogeography and the genetic legacy of aridification by explicitly testing the "out-of-Central Asia" hypothesis for the desert scorpion *M. mongolicus* in arid Central Asia (ACA). Our phylogenetic analyses of both mtCOI and nuclear genes for samples from ACA indicate that the Tian Shan-Pamir ranges largely define the distributional boundaries of various *Mesobuthus* species. This perspective is particularly well exemplified by *M. mongolicus* which is constrained in the Junggar Basin to the north of the Tian Shan and by *M. przewalskii* which is confined to the Tarim Basin to the south of the Tian Shan (Figure 1&2). Although the estimated divergence time of 10.56 Ma (95% HPD, 8.33–12.70 Ma, Table 1) between *M. mongolicus* and the *M. przewalskii* was coincident with a pulse of uplift of the Tian Shan that occurred around 10–11 Ma (Charreau et al. 2009), such a temporal match alone did not necessarily imply that the uplift of the Tian Shan had driven the divergence given the spatial mismatch between the biological event and the geological event. The ancestral populations had not reached their current distributional areas yet by the time the mountains underwent uplift (Shi et al. 2013). Nevertheless, our findings here, as well as observations from other studies in ACA (Graham et al. 2019; Zhang et al. 2020), together with evidence from geological and zoogeographical investigations (Charreau et al. 2009; Sun et al. 2015; He et al. 2020), collectively suggest that the Tian Shan mountains represent an almost insurmountable barrier to fauna exchange within ACA. However, *M. mongolicus* and its closely related lineages manifested a trans-barrier distribution with more deeply diverged lineages occurring in Central Asia and more recently derived lineages in China and Mongolia (Figure 2). The young coalescent age of *M. mongolicus* (Table 1) which postdates the uplift of the Tian Shan and Pamir implies that a corridor must have existed for this scorpion to disperse out of Central Asia (Charreau et al. 2009; Sun et al. 2015). Such a trans-barrier genetic distributional pattern is compatible with the "out-of-Central Asia" hypothesis (Shi et al. 2013).

Indeed, the results from the Bayesian phylogeographic reconstruction and population genetic analysis indicate that the Junggar Basin has severed as the corridor for *M. mongolicus* to disperse out-of-Central Asia. In northwest China and south Mongolia, *M. mongolicus* represents a coherent lineage that diverged from its most closely related lineage (TJ01) in Central Asia at about 1.36 Ma (0.78–1.97 Ma, Table 1). The ancestral population dispersed from Central Asia eastward to the Junggar Basin around 0.8 Ma, then moved further

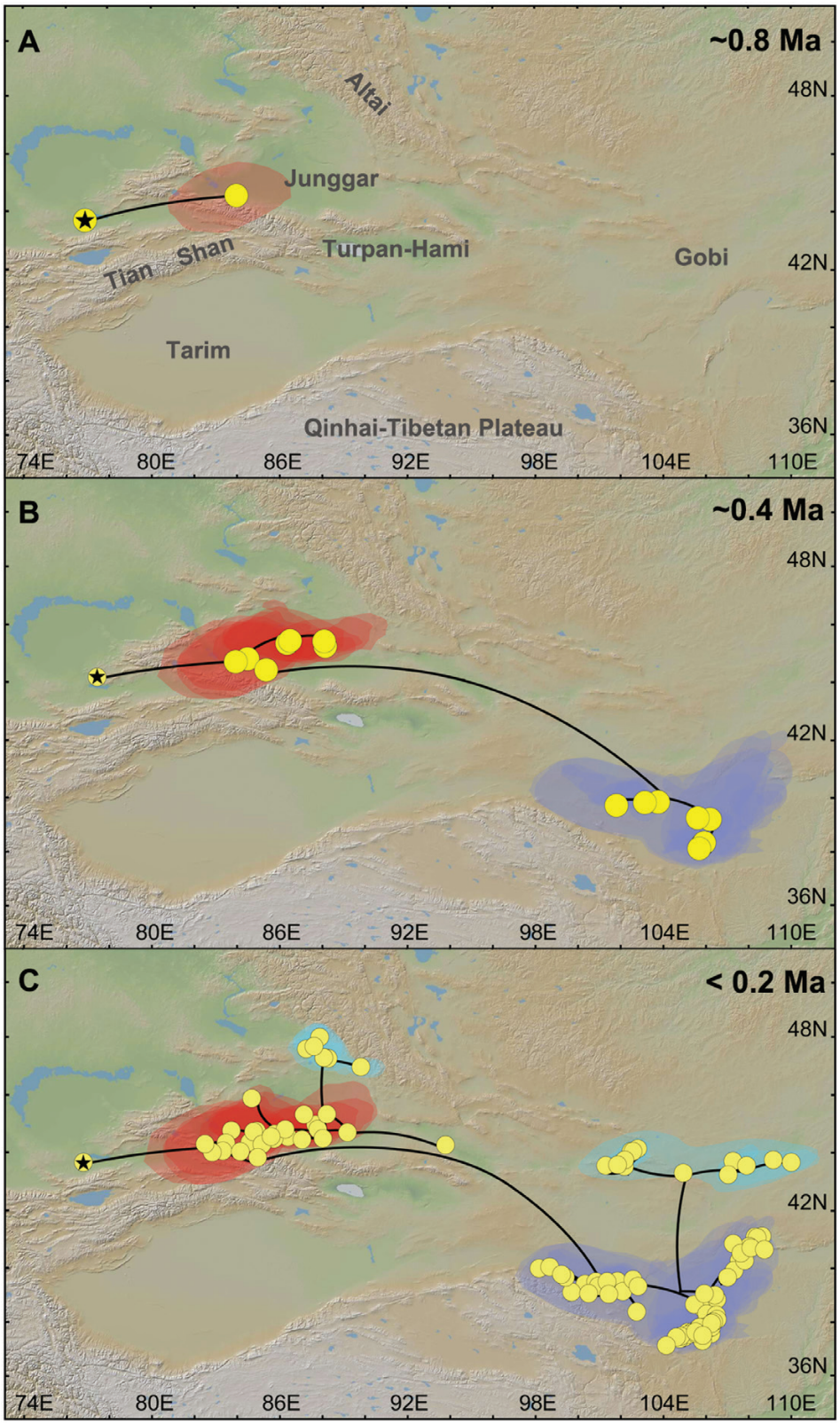

Figure 3. Spatiotemporal reconstruction of the geographic dispersal of *M. mongolicus* using Bayesian phylogeographic method. Shown here are three snapshots illustrating that *M. mongolicus* originated in Central Asia (A), then dispersed eastward step by step (B), and finally to the Gobi region (C). The geographic spread of genealogies across spaces was modeled with a continuous diffusion process governed by the relaxed random walk using the software BEAST. Yellow circles represent nodes of the maximum clade credibility phylogeny. Areas shaded in color in the background represent the 80% highest posterior density intervals which depicted the uncertainty of phylogeographic estimates for the nodes.

Table 2. Summary statistics of mtCOI data of *M. mongolicus*

	N	h	Hd	π	*D*	*Fs*	R_2
All	340	63	0.7253	0.0024	-2.4128**	-98.3099**	0.0760**
Junggar	23	10	0.8063	0.0029	-1.3799	-4.6215*	0.1378**
Gobi	317	53	0.6849	0.0020	-2.4037**	-28.8463**	0.0769**

Notes: N, sample size; h, number of haplotypes; Hd, hapotype diversity; π, nucleotide diversity; *D*, Tajima's *D* statistic; *Fs*, Fu's *Fs* statistic; R_2, Ramos-Onsins & Rozas' statistic. Asterisks * denote $P < 0.05$ and ** $P < 0.01$.

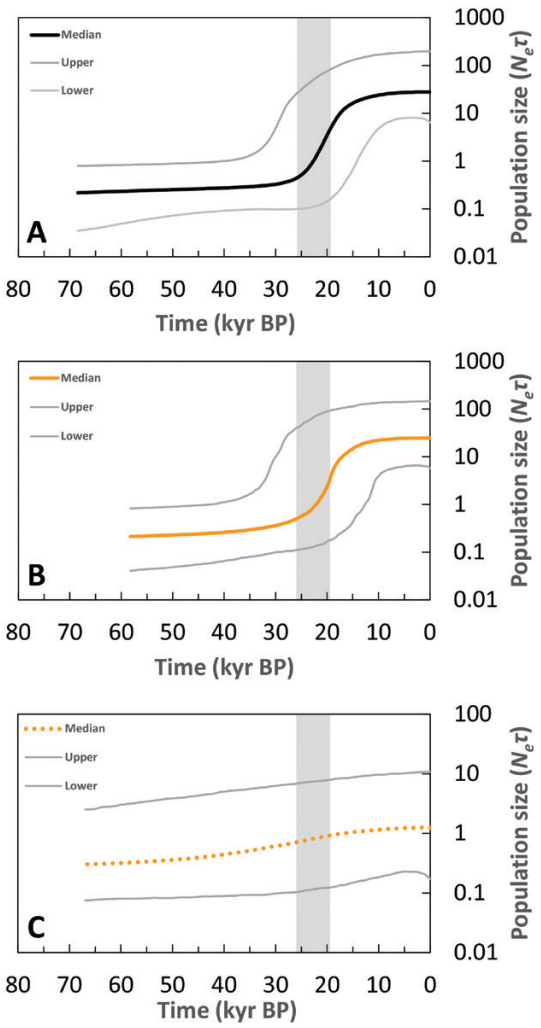

Figure 4. Demographic histories of *M. mongolicus* estimated using Bayesian skyline plots from mtCOI sequences. (A) the species as a whole, (B) the Gobi population, and (C) the Junggar population. The medians and their 95% highest posterior density intervals (gray lines) of effective population sizes were plotted against time. The *x*-axis represents time in thousand years (kyr) before the present. The *y*-axis is the log scaled effective population size ($N_e\tau$). The vertical gray bars indicate the LGM between 26.5 and 19 kyr ago.

eastward and finally reached the Gobi deserts around 0.4 Ma (Figure 3). The fading of population coalescent times and diffusion of genealogies indicated a west-east dispersal process. In addition, the summary statistics of genetic diversity (Hd and π) for the western Junggar population were significantly higher than those for the eastern Gobi population (Table 2). Such a pattern of decaying genetic diversity was consistent with a scenario of population expansion from west to east. Besides, we noticed that similar phylogeographic patterns have been reported in the agamid lizards *Phrynocephalus* sp. (Melville et al. 2009) and the rapid racerunner *Eremias velox* (Liu et al. 2019). These lines of evidence collectively suggest that the Junggar Basin has played a critical role in shaping phylogeographic patterns of arid-adapted species. While the lofty Tian Shan-Pamir ranges have formed a formidable barrier, some animals have successfully made a detour along the Junggar Basin corridor to maintain genetic exchange between Central Asia and East Asia.

The Junggar route out of Central Asia unveiled by the phylogeography of *M. mongolicus* reconciled well to the geo-climatic context of ACA. This scorpion, and the *M. eupeus* species complex in general, are typical arid-adapted species with a close affinity to various desert ecosystems (Fet et al. 2000; Shi et al. 2007; Shi et al. 2015a). Over the past 1.77 million years, the ACA has become increasingly arid, experiencing extremely dry climatic conditions in southern Tajikistan since 0.85 Ma (Ding et al. 2002; Yang and Ding 2006) and in the Junggar Basin no later than 0.8 Ma (Fang et al. 2002). It was during the mid-Pleistocene climate transition that *M. mongolicus* dispersed from its projected ancestral area in Tajikistan to the Junggar Basin (Figure 3). The subsequent expansions of deserts in the Junggar Basin at ~0.65 and 0.5 Ma (Fang et al. 2002) might have opened up abundant habitats for the proliferation of *M. mongolicus*. It was around 0.4 Ma when the arid desert landscape was fully developed on the alluvial plain of the Gobi-Altai (Lü et al. 2010), then *M. mongolicus* dispersed further eastward to the Gobi regions where Badain Jaran and Tengger Deserts were in place around 0.85 Ma (Guan et al. 2011; Li et al. 2014). It is interesting to note that the two major dispersal events occurred during interglacial periods when Earth was in a similar orbital variation of eccentricity as present-day and climatic conditions were analogous to the current status (Droxler et al. 2003). During these periods, the suitable distributional areas for *M. mongolicus* might be fully connected and become continuous similar to the present-day situation (Figure 5).

The out-of-Central Asia move of *M. mongolicus* was further sustained by population expansion during the arid glacial period. The star-shaped genealogy (Figure 2AC), the excess of rare mutations and deficit of intermediate frequency mutation (Figure 2B), and the results of Tajima's *D*, Fu's *Fs* as well as R_2 tests (Table 2), all supported population expansion for *M. mongolicus*. The results of BSP indicated that *M. mongolicus* populations underwent exponential growth throughout the LGM (Figure 3A) when the global icesheets and mountain glaciers reached their maximum volume between 26.5 and 19 ka (Clark et al. 2009). Similar trends were also observed in the desert-dwelling gerbil (Wang et al. 2013), the desert hamster (Lv et al. 2016), the rapid racerunner (Liu et al. 2019), and several desert plants

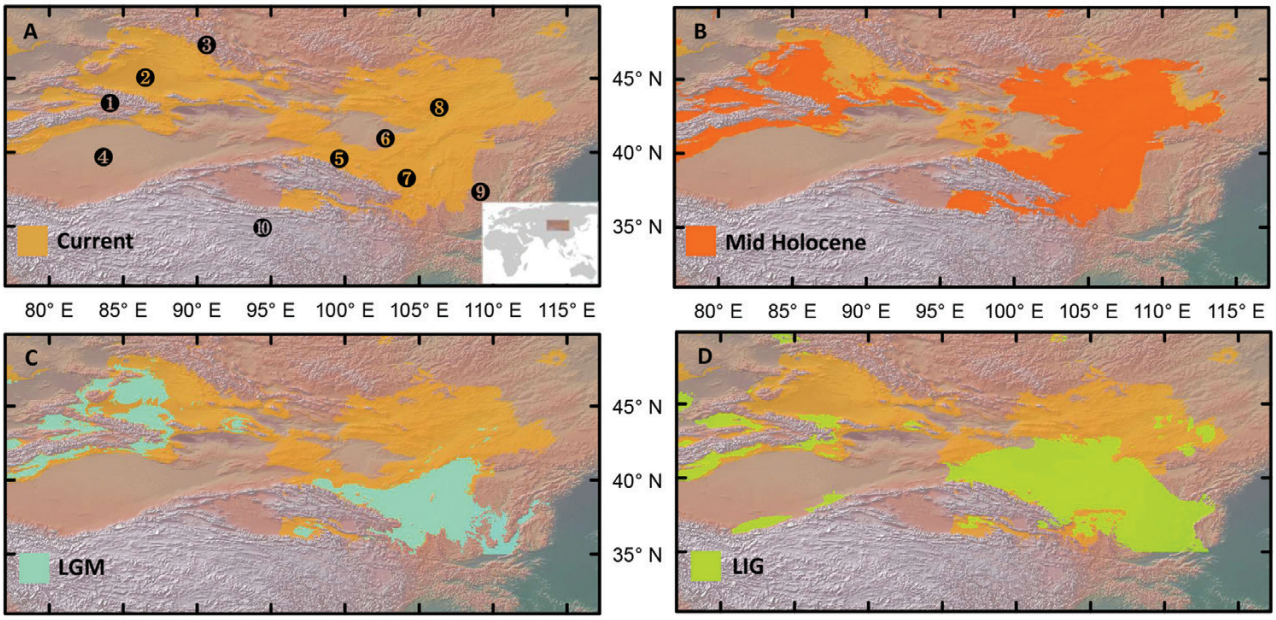

Figure 5. Potentially suitable distribution areas for *M. mongolicus* predicted by ecological niche modeling. (A) the present, (B) the Holocene, (C) the LGM, and (D) the LIG. The major geographic features discussed in the text are shown on the current model (A): ❶ Tian Shan, ❷ Junggar Basin, ❸ Altai Mountains, ❹ Tarim Basin, ❺ Hexi Corridor, ❻ Badain Jaran Desert, ❼ Tengger Desert, ❽ Gobi Desert, ❾ Loess Plateau, ❿ Qinghai-Tibetan Plateau.

(Meng and Zhang 2013; Shi and Zhang 2015) in the Gobi regions. Such a glacial expansion phenomenon is in sharp contrast to the paradigmatic interglacial-expansion and glacial-contraction model corroborated by temperate flora and fauna of North America and Europe (Hewitt 2004; Schmitt 2007). It is also inconsistent with the scenario for the mesic biota in arid regions of the other parts of the world, in which population contraction occurred during the LGM with the effect of aridification mirrored that of glaciation (Fujita et al. 2010). However, population expansion during the LGM did not appear unusual among arid-adapted species and was not limited to the Gobi deserts and adjacent regions. Similar demographic histories have been detected in arid-adapted species from other regions of the world, for instance, the grey butcherbird from southern Australia (Kearns et al. 2014), the lizard in the Monte Desert (Camargo et al. 2013), and beetles in the Sonoran Desert (Pfeiler et al. 2013). We acknowledge that the demography of glacial population expansion not only reconciles to the ecology of *M. mongolicus* but also fits well with environmental history in the Gobi regions. During the LGM, climate change in these regions seemed moderate as indicated by limited glacial expansion on the nearby mountains (Lifton et al. 2014). Thus, the stress induced by lowing temperature associated with the glacial expansion would be alleviated. In addition, as the species have well adapted to the arid environment, aridification associated with glaciation would not exert much stress on its persistence. On the contrary, the consequential expansion of desert environments might have opened up an array of new habitats for arid species (Wang et al. 2021). For example, the expansion of dune fields during glacial periods (Dong et al. 2013; Lu et al. 2013) would provide *M. mongolicus* with a suitable matrix for burrowing, by which they could effectively buffer the climate extremes. As a consequence, although the overall size of their distributional area was reduced during the LGM (Figure 5), the localized effective niche spaces might have expanded with the development of the desert ecosystems. Finally, given that *M. mongolicus* has colonized the Gobi regions rather recently (Figure 3) and that scorpions can maintain extremely high biomass in arid communities (Polis and Yamashita 1991), it could be expected that the population density would be far below the carrying capacity of the habitats even at the LGM, thus still allowing the proliferation of scorpions. Our results, along with other cases of LGM expansion in arid-adapted species, substantiate that organisms' ecological adaptation was an important determinant of their demographic response to climate changes.

Scorpions of the genus *Mesobuthus* are of great medical significance (Shi et al. 2007, 2015b; Lourenço 2018; Ward et al. 2018). Their venoms, formed by complex mixtures of highly specific toxins, have been a rich resource for bioactive molecules of pharmacal and insecticidal potentials (Goudet et al. 2002; Smith et al. 2013; Zhu et al. 2013). However, the species boundaries for many members of *Mesobuthus* remain to be robustly defined. Deep divergences of *M. mongolicus* with its parapatric species, *M. martensii* and *M. przewalskii*, both in mtCOI and nuclear genes (Figure 2A, C, Table 1) made it uncontroversial to assume them as independent species. Our phylogenetic analysis of mtCOI indicates the Chinese-Mongolian lineage formed a monophyletic clade (Figure 2A) which diverged with the Tajik lineage at least 0.8 Ma (Table 1), suggesting that they might represent an independent evolutionary unit. However, their evolutionary independency was not supported by nuclear genes (Figure 2C). The shallow divergence between the Tajik lineage (TJ01) and the Chinese-Mongolian lineage in mtCOI and their nested phylogenetic relationship in the nuclear gene tree made it impracticable to demarcate a genetic boundary for the species at present. The conflict between the mitochondrial gene tree and the nuclear gene tree needs to be explored using genome-wide data with methods that integrate the phylogenetic process of species divergences and the population genetic process of coalescence

(Shi and Yang 2017; Jiao et al. 2021). The genetic boundary of *M. mongolicus* remains to be delimitated using genome-wide data in the future.

Acknowledgements

We are grateful to the Plant Protection Research Institute, Mongolia, for logistical supports on field surveys. We thank Xian-Guang Guo, Peng He, Hong-Bin Liang, Ke-Qing Song, Zhiyuan Su, Duo-Hong Wang, Zhi-Liang Wang, and Alexander V. Gromov for providing scorpion specimens. We thank anonymous reviewers for insightful comments on previous versions of this manuscript.

Funding

This study was supported by the National Natural Science Foundation of China (grant nos. 31772435, 32170455). C.-M.S. is also supported by a starting fund from Hebei Agricultural University and the State Key Laboratory of North China Crop Improvement and Regulation (YJ2020028).

Author Contributions

D.-X.Z. and C.-M.S. conceived and designed the project; C.-M.S., X.-S.Z., L.L and Y.-J.J. collected the molecular data; C.-M.S. performed the field work and analyzed data; C.-M.S. and D.-X.Z. wrote the manuscript.

Conflict of Interest

The authors declare that they have no conflict of interest.

References

Ackerly DD, Loarie SR, Cornwell WK, Weiss SB, Hamilton H et al., 2010. The geography of climate change: Implications for conservation biogeography. *Divers Distrib* **16**:476–487.

Alqahtani AR, Badry A, Aly H, Amer SAM, Al Galil FMA et al., 2022. Genetic diversity and population structure of *Androctonus crassicauda* (Scorpiones: Buthidae) in different ecogeographical regions of Saudi Arabia and Iran. *Zool Middle East* **68**:171–179.

Anadón JD, Graciá E, Botella F, Giménez A, Fahd S et al., 2015. Individualistic response to past climate changes: Niche differentiation promotes diverging quaternary range dynamics in the subspecies of *Testudo graeca*. *Ecography* **38**:956–966.

Austin AT, 2011. Has water limited our imagination for aridland biogeochemistry? *Trends Ecol Evol* **26**:229–235.

Avise JC, Bowen BW, Ayala FJ, 2016. . In the light of evolution X: Comparative phylogeography. *Proc Natl Acad Sci* **113**:7957–7961.

Bandelt HJ, Forster P, Röhl A, 1999. Median-joining networks for inferring intraspecific phylogenies. *Mol Biol Evol* **16**:37–48.

Barbolini N, Woutersen A, Dupont-Nivet G, Silvestro D, Tardif D et al., 2020. Cenozoic evolution of the steppe-desert biome in Central Asia. *Sci Adv* **6**:eabb8227.

Bielejec F, Baele G, Vrancken B, Suchard MA, Rambaut A et al., 2016. SpreaD3: Interactive visualization of spatiotemporal history and trait evolutionary processes. *Mol Biol Evol* **33**:2167–2169.

Birula A, 1911. Arachnologische Beiträge. I. Zur Scorpionen-und Solifugen-Fauna des Chinesischen Reiches. *Revue Russe d'Entomologie* **11**:195–199.

Bougeois L, Dupont-Nivet G, de Rafélis M, Tindall JC, Proust J-N et al., 2018. Asian monsoons and aridification response to Paleogene sea retreat and Neogene westerly shielding indicated by seasonality in Paratethys oysters. *Earth Planet Sci Lett* **485**:99–110.

Bryson RW Jr, Riddle BR, Graham MR, Smith BT, Prendini L, 2013a. As old as the hills: Montane scorpions in southwestern North America reveal ancient associations between biotic diversification and landscape history. *PLoS One* **8**:e52822.

Bryson Jr RW, Savary WE, Prendini L, 2013b. Biogeography of scorpions in the *Pseudouroctonus minimus* complex (Vaejovidae) from south-western North America: Implications of ecological specialization for pre-quaternary diversification. *J Biogeogr* **40**:1850–1860.

Byrne M, Joseph L, Yeates D, Roberts J, Edwards D, 2018. Evolutionary history. In: Lambers H editor. *On the Ecology of Australia's Arid Zone*. Springer International Publishing, 45–75.

Byrne M, Yeates D, Joseph L, Kearney M, Bowler M et al., 2008. Birth of a biome: Insights into the assembly and maintenance of the Australian arid zone biota. *Mol Ecol* **17**:4398–4417.

Cain S, Loria SF, Ben-Shlomo R, Prendini L, Gefen E, 2021. Dated phylogeny and ancestral range estimation of sand scorpions (Buthidae: *Buthacus*) reveal early Miocene divergence across land bridges connecting Africa and Asia. *Mol Phylogenetics Evol* **164**:107212.

Camargo A, Werneck FP, Morando M, Sites Jr JW, Avila LJ, 2013. Quaternary range and demographic expansion of *Liolaemus darwinii* (Squamata: Liolaemidae) in the monte desert of central Argentina using Bayesian phylogeography and ecological niche modelling. *Mol Ecol* **22**:4038–4054.

Ceccarelli FS, Ojanguren-Affilastro AA, Ramírez MJ, Ochoa JA, Mattoni CI et al., 2016. Andean uplift drives diversification of the bothriurid scorpion genus *Brachistosternus*. *J Biogeogr* **43**:1942–1954.

Ceccarelli FS, Pizarro-Araya J, Ojanguren-Affilastro AA, 2017. Phylogeography and population structure of two *Brachistosternus* species (Scorpiones: Bothriuridae) from the Chilean coastal desert-the perils of coastal living. *Biol J Linn Soc* **120**:75–89.

Charreau J, Chen Y, Gilder S, Barrier L, Dominguez S et al., 2009. Neogene uplift of the Tian Shan Mountains observed in the magnetic record of the Jingou River section (northwest China). *Tectonics* **28**:n/aTC2008–n/aTC2n/a.

Chen F, Jia J, Chen J, Li G, Zhang X et al., 2016. A persistent Holocene wetting trend in arid Central Asia, with wettest conditions in the late Holocene, revealed by multi-proxy analyses of loess-paleosol sequences in Xinjiang, China. *Quat Sci Rev* **146**:134–146.

Clark PU, Dyke AS, Shakun JD, Carlson AE, Clark J et al., 2009. The last glacial maximum. *Science* **325**:710–714.

Davis M, Shaw R, 2001. Range shifts and adaptive responses to quaternary climate change. *Science* **292**:673–679.

Di Z-Y, Yang Z-Z, Yin S-J, Cao Z-J, Li W-X, 2014. History of study, updated checklist, distribution and key of scorpions (Arachnida: Scorpiones) from China. *Zool Res* **35**:3.

Ding ZL, Ranov V, Yang SL, Finaev A, Han JM et al., 2002. The loess record in southern Tajikistan and correlation with Chinese loess. *Earth Planet Sci Lett* **200**:387–400.

Dolby GA, Dorsey RJ, Graham MR, 2019. A legacy of geo-climatic complexity and genetic divergence along the lower Colorado River: Insights from the geological record and 33 desert-adapted animals. *J Biogeogr* **46**:2479–2505.

Dong Z, Qian G, Lv P, Hu G, 2013. Investigation of the sand sea with the tallest dunes on earth: China's Badain Jaran sand sea. *Earth-Sci Rev* **120**:20–39.

Dormann CF, Elith J, Bacher S, Buchmann C, Carl G et al., 2013. Collinearity: A review of methods to deal with it and a simulation study evaluating their performance. *Ecography* **36**:27–46.

Droxler AW, Alley RB, Howard WR, Poore RZ, Burckle LH, 2003. Unique and exceptionally long interglacial marine isotope stage 11: Window into earth warm future climate. Earth's Climate and Orbital Eccentricity: The Marine Isotope Stage 11 Question. p. 1–14.

Edgar RC, 2004. Muscle: Multiple sequence alignment with high accuracy and high throughput. *Nucleic Acids Res* **32**:1792–1797.

Fang X, Shi Z, Yang S, Yan M, Li J et al., 2002. Loess in the Tian Shan and its implications for the development of the Gurbantunggut desert and drying of northern Xinjiang. *Chin Sci Bull* **47**:1381–1387.

Fet V, 1994. Fauna and zoogeography of scorpions (Arachnida: Scorpions) in Turkmenistan. In: Fet V, Atamuradov K, eds.

Biogeography and Ecology of Turkmenistan. The Netherland: Kluwer Academic Publishers, 525–534.

Fet V, Kovařík F, Gantenbein B, Graham MR, 2021. Three new species of *Olivierus* (Scorpiones: Buthidae) from Kazakhstan and Uzbekistan. *Zootaxa* **5006**:54–72.

Fet V, Kovařík F, Gantenbein B, Kaiser R, Stewart A et al., 2018. Revision of the *Mesobuthus caucasicus* complex from Central Asia, with descriptions of six new species (Scorpiones: Buthidae). . *Euscorpius* **255**:1–77.

Fet V, Sissom W, Lowe G, Braunwalder M, 2000. *Catalog of the Scorpions of the World (1758-1998)*. New York: The New York Entomological Society.

Fick SE, Hijmans RJ, 2017. WorldClim 2: New 1km spatial resolution climate surfaces for global land areas. *Int J Climatol* **37**:4302–4315.

Fu YX, 1997. Statistical tests of neutrality of mutations against population growth, hitchhiking and background selection. *Genetics* **147**:915–925.

Fujita MK, McGuire JA, Donnellan SC, Moritz C, 2010. Diversification and persistence at the arid-monsoonal interface: Australia-wide biogeography of the Bynoe's gecko (*Heteronotia binoei*; Gekkonidae). *Evolution* **64**:2293–2314.

Gantenbein B, Fet V, Gromov AV, 2003. The first DNA phylogeny of four species of Mesobuthus (Scorpiones, Buthidae) from Eurasia. *J Arachnol* **31**:412–420.

Gantenbein B, Largiadèr CR, 2002. *Mesobuthus gibbosus* (Scorpiones: Buthidae) on the island of Rhodes-hybridization between Ulysses' stowaways and native scorpions? *Mol Ecol* **11**:925–938.

Garcia RA, Cabeza M, Rahbek C, Araújo MB, 2014. Multiple dimensions of climate change and their implications for biodiversity. *Science* **344**:1247579.

Goudet C, Chi C-W, Tytgat J, 2002. An overview of toxins and genes from the venom of the Asian scorpion *Buthus martensi* Karsch. *Toxicon* **40**:1239–1258.

Graham MR, Jaeger JR, Prendini L, Riddle BR, 2013a. Phylogeography of Beck's desert scorpion *Paruroctonus becki* reveals Pliocene diversification in the eastern California shear zone and postglacial expansion in the Great Basin Desert. *Mol Phylogenetics Evol* **69**:502–513.

Graham MR, Jaeger JR, Prendini L, Riddle BR, 2013b. Phylogeography of the Arizona hairy scorpion *Hadrurus arizonensis* supports a model of biotic assembly in the Mojave Desert and adds a new Pleistocene refugium. *J Biogeogr* **40**:1298–1312.

Graham MR, Myers EA, Kaiser RC, Fet V, 2019. Cryptic species and co-diversification in sand scorpions from the Karakum and Kyzylkum deserts of Central Asia. *Zool Scr* **48**:801–812.

Graham MR, Oláh-Hemmings V, Fet V, 2012. Phylogeography of co-distributed dune scorpions identifies the Amu Darya river as a long-standing component of Central Asian biogeography. *Zool Middle East* **55**:95—110.

Guan Q, Pan B, Li N, Zhang J, Xue L, 2011. Timing and significance of the initiation of present day deserts in the northeastern Hexi Corridor, China. *Palaeogeogr Palaeoclimatol Palaeoecol* **306**:70–74.

Guindon S, Dufayard J-F, Lefort V, Anisimova M, Hordijk W et al., 2010. New algorithms and methods to estimate maximum-likelihood phylogenies: Assessing the performance of PhyML 3.0. *Syst Biol* **59**:307–321.

Guo ZT, Ruddiman WF, Hao QZ, Wu HB, Qiao YS et al., 2002. Onset of Asian desertification by 22 myr ago inferred from loess deposits in China. *Nature* **416**:159–163.

He J, Lin S, Li J, Yu J, Jiang H, 2020. Evolutionary history of zoogeographical regions surrounding the Tibetan Plateau. *Commun Biol* **3**:415.

Hewitt G, 2000. The genetic legacy of the quaternary ice ages. *Nature* **405**:907–913.

Hewitt GM, 2004. The structure of biodiversity-insights from molecular phylogeography. *Front Zool* **1**:4.

Hijmans RJ, Cameron SE, Parra JL, Jones PG, Jarvis A, 2005. Very high resolution interpolated climate surfaces for global land areas. *Int J Climatol* **25**:1965–1978.

Ho SYW, Shapiro B, 2011. Skyline-plot methods for estimating demographic history from nucleotide sequences. *Mol Ecol Resour* **11**:423–434.

Holt BG, Lessard J-P, Borregaard MK, Fritz SA, Araújo MB et al., 2013. An update of Wallace's zoogeographic regions of the world. *Science* **339**:74–78.

Jiao X, Flouri T, Yang Z, 2021. Multispecies coalescent and its applications to infer species phylogenies and cross-species gene flow. *Natl Sci Rev* **8**:nwab127.

Jiménez-Valverde A, Lobo JM, 2007. Threshold criteria for conversion of probability of species presence to either-or presence-absence. *Acta Oecol* **31**:361–369.

Kaya F, Bibi F, Žliobaitė I, Eronen JT, Hui T et al., 2018. The rise and fall of the old world savannah fauna and the origins of the African savannah biome. *Nat Ecol Evol* **2**:241–246.

Kearns AM, Joseph L, Toon A, Cook LG, 2014. Australia's arid-adapted butcherbirds experienced range expansions during Pleistocene glacial maxima. *Nat Commun* **5**:3994.

Keppel G, Van Niel KP, Wardell-Johnson GW, Yates CJ, Byrne M et al., 2012. Refugia: Identifying and understanding safe havens for biodiversity under climate change. *Glob Ecol Biogeogr* **21**:393–404.

Knowles LL, 2009. Statistical phylogeography. *Annu Rev Ecol Evol Syst* **40**:593–612.

Kovařík F, 2019. Taxonomic reassessment of the genera *Lychas*, *Mesobuthus*, and *Olivierus*, with descriptions of four new genera (Scorpiones: Buthidae). *Euscorpius* **288**:1–27.

Kovařík F, Fet V, Gantenbein B, Graham M, Yağmur E et al., 2022. A revision of the genus *Mesobuthus* Vachon, 1950, with a description of 14 new species (Scorpiones: Buthidae). *Euscorpius* **348**:1–189.

Kreft H, Jetz W, 2010. A framework for delineating biogeographical regions based on species distributions. *J Biogeogr* **37**:2029–2053.

Lemey P, Rambaut A, Welch JJ, Suchard MA, 2010. Phylogeography takes a relaxed random walk in continuous space and time. *Mol Biol Evol* **27**:1877–1885.

Li Z, Sun D, Chen F, Wang F, Zhang Y et al., 2014. Chronology and paleoenvironmental records of a drill core in the central Tengger desert of China. *Quat Sci Rev* **85**:85–98.

Lifton N, Beel C, Hättestrand C, Kassab C, Rogozhina I et al., 2014. Constraints on the late quaternary glacial history of the Inylchek and Sary-Dzaz valleys from *in situ* cosmogenic ^{10}Be and ^{26}Al, eastern Kyrgyz Tian Shan. *Quat Sci Rev* **101**:77–90.

Liu J, Guo X, Chen D, Li J, Yue B et al., 2019. Diversification and historical demography of the rapid racerunner *Eremias velox* in relation to geological history and Pleistocene climatic oscillations in arid Central Asia. *Mol Phylogenetics Evol* **130**:244–258.

Lourenço WR, 2018. The evolution and distribution of noxious species of scorpions (Arachnida: Scorpiones). *JVATiTD* **24**:1.

Lu H, Yi S, Xu Z, Zhou Y, Zeng L et al., 2013. Chinese deserts and sand fields in Last Glacial Maximum and Holocene Optimum. *Chin Sci Bull* **58**:2775–2783.

Lü Y, Gu Z, Aldahan A, Zhang H, Possnert G et al., 2010. . ^{10}Be in quartz gravel from the Gobi desert and evolutionary history of alluvial sedimentation in the Ejina Basin, Inner Mongolia, China. *Chin Sci Bull* **55**:3802–3809.

Lv X, Xia L, Ge D, Wen Z, Qu Y et al., 2016. Continental refugium in the Mongolian Plateau during Quaternary glacial oscillations: Phylogeography and niche modelling of the endemic desert hamster *Phodopus roborovskii*. *PLoS One* **11**:e0148182.

Maestre FT, Benito BM, Berdugo M, Concostrina-Zubiri L, Delgado-Baquerizo M et al., 2021. Biogeography of global drylands. *New Phytol* **231**:540–558.

McCormick S, Polis G, 1990. Prey, predators, and prarasites. In: Polis G editor. *The Biology of Scorpions*. Stanford: Stanford University Press, p. 145–157.

Melville J, Hale J, Mantziou G, Ananjeva NB, Milto K et al., 2009. Historical biogeography, phylogenetic relationships and intraspecific diversity of agamid lizards in the Central Asian deserts of Kazakhstan and Uzbekistan. *Mol Phylogenetics Evol* **53**:99–112.

Meng H-H, Zhang M-L, 2013. Diversification of plant species in arid northwest China: Species-level phylogeographical history of *Lagochilus bunge ex bentham* (Lamiaceae). *Mol Phylogenetics Evol* **68**:398–409.

Merow C, Smith MJ, SilanderJA Jr, 2013. A practical guide to maxent for modeling species' distributions: What it does, and why inputs and settings matter. *Ecography* **36**:1058–1069.

Miller AL, Makowsky RA, Formanowicz DR, Prendini L, Cox CL, 2014. Cryptic genetic diversity and complex phylogeography of the boreal North American scorpion *Paruroctonus boreus* (Vaejovidae). *Mol Phylogenetics Evol* **71**:298–307.

Mirshamsi O, Sari A, Elahi E, Hosseinie S, 2010. Phylogenetic relationships of *Mesobuthus eupeus* (C. L. Koch, 1839) inferred from COI sequences (Scorpiones: Buthidae). *J Nat Hist* **44**:2851–2872.

Mirshamsi O, Sari A, Elahi E, Hosseinie S, 2011. *Mesobuthus eupeus* (Scorpiones: Buthidae) from Iran: A polytypic species complex. *Zootaxa* **2929**:1–21.

Naimi B, Hamm NAS, Groen TA, Skidmore AK, Toxopeus AG, 2014. Where is positional uncertainty a problem for species distribution modelling? *Ecography* **37**:191–203.

Pannell JR, 2003. Calescence in metapopulation with recurrent local extinction and recolonization. *Evolution* **57**:949–961.

Peel MC, Finlayson BL, McMahon TA, 2007. Updated world map of the Köppen-Geiger climate classification. *Hydrol Earth Syst Sci* **11**:1633–1644.

Pepper M, Keogh JS, 2021. Life in the "dead heart" of Australia: The geohistory of the Australian deserts and its impact on genetic diversity of arid zone lizards. *J Biogeogr* **48**:716–746.

Peterson AT, Soberón J, Pearson RG, Anderson RP, Martínez-Meyer E et al., 2011. *Ecological Niches and Geographic Distributions*. Princeton: Princeton University Press.

Pfeiler E, Johnson S, Richmond MP, Markow TA, 2013. Population genetics and phylogenetic relationships of beetles (Coleoptera: Histeridae and Staphylinidae) from the Sonoran Desert associated with rotting columnar cacti. *Mol Phylogenetics Evol* **69**:491–501.

Phillips SJ, Anderson RP, Schapire RE, 2006. Maximum entropy modeling of species geographic distributions. *Ecol Modell* **190**:231–259.

Polis G, 1990. *The Biology of Scorpions*. Stanford: Stanford University Press.

Polis G, Yamashita T, 1991. The ecology and importance of predaceous arthropods in desert communities. In: Polis G editor. *The Ecology of Desert Communities*. Tucson: The University of Arizona Press, 180–222.

Posada D, Crandall KA, 1998. Modeltest: Testing the model of DNA substitution. *Bioinformatics* **14**:817–818.

Rambaut A, Drummond AJ, Xie D, Baele G, Suchard MA, 2018. Posterior summarization in Bayesian phylogenetics using tracer 1.7. *Syst Biol* **67**:901–904.

Ramos-Onsins SE, Rozas J, 2002. Statistical properties of new neutrality tests against population growth. *Mol Biol Evol* **19**:2092–2100.

Reynolds JF, Smith DMS, Lambin EF, Turner BL, Mortimore M et al., 2007. Global desertification: Building a science for dryland development. *Science* **316**:847–851.

Ronquist F, Teslenko M, van der Mark P, Ayres DL, Darling A et al., 2012. MrBayes 3.2: Efficient Bayesian phylogenetic inference and model choice across a large model space. *Syst Biol* **61**:539–542.

Rozas J, Ferrer-Mata A, Sánchez-DelBarrio JC, Guirao-Rico S, Librado P et al., 2017. . DnaSP 6: DNA sequence polymorphism analysis of large data sets. *Mol Biol Evol* **34**:3299–3302.

Schimel DS, 2010. Drylands in the Earth system. *Science* **327**:418–419.

Schmitt T, 2007. Molecular biogeography of Europe: Pleistocene cycles and postglacial trends. *Front Zool* **4**:11.

Sharma PP, Fernández R, Esposito LA, González-Santillán E, Monod L, 2015. Phylogenomic resolution of scorpions reveals multilevel discordance with morphological phylogenetic signal. *Proc R Soc Lond B Biol Sci* **282**:20142953.

Shi C-M, Huang Z-S, Wang L, He L-J, Hua Y-P et al., 2007. Geographical distribution of two species of *Mesobuthus* (Scorpiones: Buthidae) in China: Insights from systematic field survey and predictive models. . *J Arachnol* **35**:215–226.

Shi C-M, Ji Y-J, Liu L, Wang L, Zhang D-X, 2013. Impact of climate changes from middle Miocene onwards on evolutionary diversification in Eurasia: Insights from the mesobuthid scorpions. *Mol Ecol* **22**:1700–1716.

Shi C-M, Liang H-B, Altanchimeg D, Chuluunjav C, Nonnaizab et al., 2015a. Climatic niche defines geographical distribution of *Mesobuthus eupeus mongolicus* (Scorpiones: Buthidae) in Gobi desert. *Zool Syst* **40**:339–348.

Shi C-M, Yang Z, 2017. Coalescent-based analyses of genomic sequence data provide a robust resolution of phylogenetic relationships among major groups of gibbons. *Mol Biol Evol* **35**:159–179.

Shi C-M, Zhang D-X, 2005. A review of the systematic research on buthid scorpions (Scorpiones, Buthidae). *Acta Zootaxonomica Sinica* **30**:470–477.

Shi C-M, Zhang X-S, Zhang D-X, 2015b. Parasitoidism of the *Sarcophaga dux* (Diptera: Sarcophagidae) on the *Mesobuthus martensii* (Scorpiones: Buthidae) and its implications. *Ann Entomol Soc Am* **108**:978–985.

Shi X-J, Zhang M-L, 2015. Phylogeographical structure inferred from CpDNA sequence variation of *Zygophyllum xanthoxylon* across north-west China. *J Plant Res* **128**:269–282.

Sissom W, 1990. Systematics, biogeography, and paleontology. In: Polis G editor. *The Biology of Scorpions*. Standord: Stanford University Press, 64–160.

Smith JJ, Herzig V, King GF, Alewood PF, 2013. The insecticidal potential of venom peptides. *Cell Mol Life Sci* **70**:3665–3693.

Strimmer K, Pybus OG, 2001. Exploring the demographic history of DNA sequences using the generalized skyline plot. *Mol Biol Evol* **18**:2298–2305.

Suchard MA, Lemey P, Baele G, Ayres DL, Drummond AJ et al., 2018. Bayesian phylogenetic and phylodynamic data integration using BEAST 1.10. *Virus Evol* **4**:vey016.

Sun J, Gong Z, Tian Z, Jia Y, Windley B, 2015. Late Miocene stepwise aridification in the Asian interior and the interplay between tectonics and climate. *Palaeogeogr Palaeoclimatol Palaeoecol* **421**:48–59.

Sun J, Windley BF, 2015. Onset of aridification by 34 Ma across the Eocene-Oligocene transition in central Asia. *Geology* **43**:1015–1018.

Swets JA, 1988. Measuring the accuracy of diagnostic systems. *Science* **240**:1285–1293.

Tajima F, 1989. Statistical method for testing the neutral mutation hypothesis by DNA polymorphism. *Genetics* **123**:585–595.

Tietjen B, Jeltsch F, Zehe E, Classen N, Groengroeft A et al., 2010. Effects of climate change on the coupled dynamics of water and vegetation in drylands. *Ecohydrology* **3**:226–237.

Wang C, Wang X, Liu D, Wu H, Lü X et al., 2014. Aridity threshold in controlling ecosystem nitrogen cycling in arid and semi-arid grasslands. *Nat Commun* **5**:4799.

Wang F, Li Z, Sun X, Li B, Wang X et al., 2021. A 1200 ka stable isotope record from the center of the Badain Jaran desert, northwestern China: Implications for the variation and interplay of the westerlies and the Asian summer monsoon. *Geochem Geophys Geosyst* **22**:e2020GC009575.

Wang W, Liu G-M, Zhang D-X, 2019. Intraspecific variation in metabolic rate and its correlation with local environment in the Chinese scorpion *Mesobuthus martensii*. *Biol Open* **8**:bio041533.

Wang Y, Zhao L-M, Fang F-J, Liao J-C, Liu N-F, 2013. Intraspecific molecular phylogeny and phylogeography of the *Meriones meridianus* (Rodentia: Cricetidae) complex in northern China reflect the processes of desertification and theTianshan Mountains uplift. *Biol J Linn Soc* **110**:362–383.

Ward MJ, Ellsworth SA, Nystrom GS, 2018. A global accounting of medically significant scorpions: Epidemiology, major toxins, and comparative resources in harmless counterparts. *Toxicon* **151**:137–155.

Willis KJ, Bennett KD, Walker D, Hewitt GM, 2004. Genetic consequences of climatic oscillations in the quaternary. *Philos Trans R Soc Lond B Biol Sci* **359**:183–195.

Yang S, Ding Z, 2006. Winter-spring precipitation as the principal control on predominance of C_3 plants in central Asia over the past 1.77 myr: Evidence from $\delta^{13}C$ of loess organic matter in Tajikistan. *Palaeogeogr Palaeoclimatol Palaeoecol* **235**:330–339.

Zhang D-X, Hewitt GM, 1998. Isolation of animal cellular total DNA. In: Karp A, Isaac P, Ingram D eds. *Molecular Tools for Screening Biodiversity: Plants and Animals*. London: Chapman & Hall, 5–9.

Zhang X, Liu G, Feng Y, Zhang D, Shi C, 2020. Genetic analysis and ecological niche modeling delimit species boundary of the Przewalski's scorpion (Scorpiones: Buthidae) in arid Asian inland. *Zool Syst* **45**:81–96.

Zhu L, Peigneur S, Gao B, Tytgat J, Zhu S, 2013. Two recombinant α-like scorpion toxins from *Mesobuthus eupeus* with differential affinity toward insect and mammalian Na^+ channels. *Biochimie* **95**:1732–1740.